American Mineralogist, Volume 89, pages 438–445, 2004

Microstructural study of synthetic sintered diamond and comparison with carbonado, a natural polycrystalline diamond

SUBARNAREKHA DE,[1,*] PETER J. HEANEY,[2] YINGWEI FEI,[3] AND EDWARD P. VICENZI[4]

[1]Exobiology Branch, NASA Ames Research Center, Moffett Field, California 94035-1000, U.S.A.
[2]Department of Geosciences, Pennsylvania State University, University Park, Pennsylvania 16802, U.S.A.
[3]Geophysical Laboratory, Carnegie Institution of Washington, 5251 Broad Branch Road NW, Washington, D.C. 20015, U.S.A.
[4]Department of Mineral Sciences, Smithsonian Institution, Washington, D.C. 20560, U.S.A

ABSTRACT

Efforts to simulate the extreme toughness of the polycrystalline diamond variety known as carbonado typically entail the sintering of diamond powders in the presence of metal solvent-catalysts. In this study, we have attempted to duplicate the carbonado microstructure by sintering diamond powders without catalysts in a multi-anvil press at pressures of 6 to 9 GPa, temperatures of 1200 to 1800 °C, and times up to 6 h. The resultant microstructural defect assemblages for each experimental condition were characterized by transmission electron microscopy (TEM). Despite the absence of catalysts, sintered compacts were successfully produced for all runs, though intergranular porosity was significantly higher than that observed in natural carbonado. Primary grain sizes were reduced by more than 50% from their original dimensions in some experiments due to surface fracturing and abrasion, and aperiodic slip planes rigorously parallel to {111} consistently emerged in high densities, with lamellar spacings of 3 to 30 nm. In addition, sintering over all conditions produced polysynthetic spinel twinning in close association with the partial slip defects.

Compacts compressed at 8 GPa produced some euhedral crystals with very low dislocation densities surrounded by grains in which dislocation densities were quite high. In addition, curviplanar defects loosely constrained to {111} were visible within some specimens sintered at the highest pressures. These textures resembled the polygonalization fabrics and defect microstructures observed in natural carbonado (De et al. 1998), and the appearance of these features suggests that our experiments at their most extreme pressure and temperature parameters reproduced carbonado-like defect assemblages. The formation of such textures in quasi-hydrostatic experiments suggests that shock metamorphism is not required to produce the periodic defect lamellae observed in carbonado.

INTRODUCTION

Natural polycrystalline diamond (PCD) abrasives have long been used for cutting and drilling very hard materials, and scientists continue to explore methods of replicating the properties of carbonado, one of the more industrially important varieties of PCD. Carbonado occurs as black, irregularly shaped, polycrystalline aggregates with grain sizes ranging from less than 1 to several hundred μm (Dismukes et al. 1988; Jeynes 1978; Trueb and de Wys 1971). Unlike non-porous microcrystalline diamond aggregates found in kimberlites (e.g., stewartite and framesite), carbonado is recovered only from alluvial deposits in Brazil and the Central African Republic (CAR). Carbonado exhibits the extreme hardness and high thermal conductivity of single-crystal diamond, but it is much less vulnerable to catastrophic cleavage. The random crystallographic orientation that is typical of carbonado and other natural and synthetic polycrystalline diamond combines with a complex defect microstructure to minimize crack propagation (Lammer 1988; Wentorf et al. 1980). In addition, grinding materials composed of PCD tend to wear more uniformly than single-crystal diamond, whose hardness varies with crystallographic orientation.

Since the tight diamond-diamond bonding in carbonado suggests that it is a naturally "sintered" diamond (Hall 1970), we have attempted to reproduce the microstructural defect assemblages that are characteristic of carbonado by artificially sintering diamond powders without the use of catalysts. From experiments that yield synthetic diamonds with microstructures that are comparable to those in carbonado, we may be able to infer the temperature-pressure regime in which carbonado crystallized and developed during its genesis. Since the formation mechanism of carbonado is not yet known and highly controversial, such results would constrain the field of permissible hypotheses (Frantesson and Kaminsky 1974; Smith and Dawson 1985; Ozima et al. 1991; Kagi et al. 1994; Shelkov et al. 1995; Haggerty 1996; Ozima and Tatsumoto 1997; Shelkov et al. 1997, 1998; De et al. 1998). In addition, such studies may provide us with new insights into the mechanisms by which pure diamond powders sinter at high pressures.

SYNTHESIS OF SINTERED DIAMOND: PREVIOUS WORK

Diamond was synthesized in 1955 using molten metallic catalysts such as Mn, Cr, Ta, Fe, Ni, and their alloys in a high pressure apparatus at *P-T* conditions under which diamond is stable (Bundy et al. 1955). Since then, scientists have developed numerous methods of producing single-crystal diamonds at high pressures (Bundy et al. 1955; Liander and Lundblad 1960; Bundy 1962; Giardini and Tydings 1962; Naka et al. 1976; Wentorf et al. 1980; Slobodskoi et al. 1990; Yu and Li 1994; Zhang et al.

* E-mail: sde@alumni.princeton.edu

1994; Klages 1995; DeCarli 1995, 1998; DeVries et al. 1996) and low pressures (Angus and Hayman 1988; Williams and Glass 1989). A recent paper reports the first successful synthesis of polycrystalline sintered diamond by direct conversion of graphite under static high pressure and temperature (Irifune et al. 2003). The first sintered polycrystalline diamond with diamond powder as the starting material was produced at pressures of 6.5 to 8.5 GPa and temperatures of approximately 2500 K, and the compact was termed "carbonado" by Hall (1970). However, the author did not discuss in detail the microstructures that characterized this synthetic polycrystalline diamond, and the extent to which this material simulated natural carbonado is not clear.

During the artificial sintering process, small particles bond to form a larger coherent aggregate and the total area of contact between the diamond particles increases as the total volume of the mass shrinks. Since the hard diamond particles do not pulverize easily, it is difficult to achieve the high pressures necessary for diamond cementation over the entire surfaces of the consolidating particles (Wentorf et al. 1980). Several authors have observed that such particles sustain very high local pressures where they come in contact with each other, but the pressure over their surfaces in the interstitial voids is very low (Wentorf et al. 1980; Walmsley and Lang 1983; Walmsley and Lang 1988). Consequently, if the overall pressure is not sufficiently high, the low-pressure voids fill with low-density graphite. By contrast, when the dissolved carbon within the intergranular volumes is at high pressure and temperature, the carbon precipitates as diamond, leading to considerable intergrowth between the original diamond grains and effectively forming a dense diamond compact. These diamond compacts show characteristic microstructures that depend on the specific synthesis conditions.

Microstructures in sintered diamond

Though several researchers (Hall 1970; Bundy 1974; Wentorf et al. 1980; Walmsley and Lang 1983; Yazu et al. 1983; Zhutong et al. 1983; Walmsley and Lang 1988; Hong et al. 1991; Britun et al. 1992; Yu and Li 1994; Zhang et al. 1994) have examined various aspects of the sintering process, a systematic study of the evolution of microstructures in sintered diamond remains unavailable, because different scientists have employed different sintering temperatures, pressures, times, grain sizes, and catalysts in their experiments. As Wentorf et al. (1980) note, the stronger and more successful man-made sintered diamond compacts are brittle, two-phase materials in which 90% of the volume comprises randomly oriented diamond and the remaining 10% consists of a metallic phase. Microscopic observations of the grain boundaries suggest that the diamond grains are directly bonded to each other. The diamond-to-diamond bonding makes the sintered compact very hard and tough. However, the sintered diamond compacts contain high concentrations of defects.

Deformation twins typically are present in sintered diamond grains due to the application of a shear stress. When diamond is deformed under conditions that inhibit brittle fracture, it tends to twin along {111} because these twin composition planes minimize the energy of misfit (Hornstra 1957). Wentorf et al. (1980) note that the deformation twins are visible after relief polishing, which accentuates the greater wear resistance of the twinned region compared to the rest of the diamond crystal. This type of deformation structure is present in higher concentrations when the diamond grains are less than 1 μm in size. Wentorf et al. (1980) also suggest that if the conditions are semihydrostatic, as might be the case in the presence of a softer phase, the deformation microstructure will probably not be generated everywhere in the compacted aggregate.

Planar defects have been studied using TEM by Walmsley and Lang (1983) in sintered diamond compacts with initial monodisperse grain sizes of 30 to 40 μm with Co as the binding agent. The authors state that at pressures of approximately 6 GPa and temperatures above 1400 °C, slip on $(\bar{1}11)$ and $(1\bar{1}1)$ is common, and regions of high dislocation densities are observed. Microtwins parallel to $(\bar{1}11)$ and $(1\bar{1}1)$ also are very common in the diamond grains. On the other hand, Yazu et al. (1983) report no evidence for twins based on their TEM study of sintered diamond compacts. As the study by Yazu et al. (1983) employed separate experiments with monodispersed powders with grain sizes between 0.3 and 7 μm, Walmsley and Lang (1983) concluded that grain size is a significant factor in the generation of twins.

Consequently, Walmsley and Lang (1988) proceeded to examine diamonds with monodispersed grain sizes of 2, 10, and 25 μm synthesized using a Co catalyst at 6 GPa and above 1400 °C. The temperature and pressure conditions were very similar to the experimental conditions employed by Yazu et al. (1983) except for the larger grain size of the initial diamond powder. Interestingly, Walmsley and Lang (1988) report that their regrown diamond was virtually undeformed. The dislocation density was quite low, and most of the dislocations were associated with Co inclusions that were trapped by the advancing diamond growth front or trapped at the interface between the original and regrown diamond. Less common were graphite inclusions, which tended to be randomly oriented. Additionally, the authors found few differences in the characteristics of regrown diamond in compacts with various monodispersed grain size distributions. Because diamond-to-diamond bonding was pervasive in these sintered compacts, their mechanical properties were similar to those of the individual original particles.

For our study, we employed no metal catalysts and thus the synthesis procedure differed from those previously employed for the manufacture of polycrystalline diamond compacts. Moreover, our investigations were designed to examine in a systematic way the effects that variations in temperature, pressure, and sintering times exert on the microstructures of synthetic polycrystalline diamond within the constraints imposed by the experimental difficulties of these high pressures and temperatures.

Experimental procedures

Synthesis of diamonds

Experiments were performed in a multi-anvil press at the Geophysical Laboratory, Carnegie Institution of Washington, D.C. All experiments employed an 18/11 assembly, in which a ceramic MgO octahedron with an 18 mm edge length served as the pressure medium and eight tungsten carbide cubes with a corner truncation of 11 mm applied pressure on the cell. A full description of the sample assemblies and the multianvil apparatus is given in Bertka and Fei (1996, 1997). We employed diamond powders from two different manufacturers: GE Superabrasives and DuPont Beta Diamond Products. Diamond grain sizes with diameters of 5 to 7 μm from GE Superabrasives had a normal distribution of grain sizes with a mean of 6 μm and a standard deviation of 1 μm. Diamond grains from DuPont Beta Diamond Products (4 to 8 μm in diameter) had a normal distribution of grain

sizes with a mean of 6 μm and a standard deviation of 2 μm (as specified by the manufacturers and confirmed by our TEM examination). The powdered samples, without any catalysts, were sealed in molybdenum capsules. The capsules (0.5–1 mm in diameter by 3–4 mm in length) for this assembly were separated from a graphite heater by an MgO sleeve.

Temperatures were measured using a W5%Re-W26%Re thermocouple. The samples were fully pressurized at a rate of 1 GPa/hour and then heated at 80 °C/min. Experiments were terminated by cutting power to the furnace to thermally quench the samples, then allowing the samples to slowly depressurize. Detailed descriptions of the pressure-temperature-time conditions for each run are presented in Table 1.

Transmission electron microscopy

The preparation of ion-thinned samples for TEM was designed to avoid contamination by lapidary diamond. Petrographic thin sections of sintered diamond specimens were polished with a 220 mesh, 8-inch diamond lap, which was chosen for the large size (~60 μm) of its natural abrasive and was bruted smooth with a diamond tool. This hard non-abrasive surface then was used as a slow speed (400 rpm) mud lap with boron carbide loose abrasive in extra virgin olive oil. Once the sample sections were 40 μm thick, they were thinned for 40 to 80 h by Ar ion bombardment using a Gatan ion mill. Because of the very small sample volumes (mm^3) and the hardness of the materials, preparation of foils that were uniformly electron transparent was very difficult. The samples were carbon coated and examined with Philips 420, Hitachi 2000, and Philips CM 200 FEG transmission electron microscopes.

Results

Sintered diamond experiments

TEM examination of the starting powders revealed virtually no evidence for dislocations, stacking faults, or twin boundaries, thereby confirming the high degree of crystallinity of the initial material. Grain sizes were seen to be monodispersed within the 4 to 8 μm and 5 to 7 μm ranges as specified by the manufacturers, and grain shapes varied from anhedral to subhedral. A discussion of the microstructures produced in sintered diamond as a function of maximum temperature, pressure, and sintering times follows.

Variations in microstructure with sintering temperature

Diamond powders with starting sizes of 5 to 7 μm were sintered at 6 GPa and 1200, 1600, and 1800 °C for 6, 3, and 3 h, respectively. The experiment at 1800 °C "blew out" after 3 h and produced very different textures from those seen in diamonds from the lower-temperature runs (discussed below). In the experiments at 1200 and 1600 °C, the mean particle sizes decreased from their original dimensions, and the synthetic diamond compacts consisted of particles ranging from 0.2 to 4 μm in size (Fig. 1). Grains were incompletely consolidated with abundant gaps at grain boundaries. Tiny tabular (160 nm × 900 nm) and acicular (30 nm × 260 nm) diamond crystallites frequently could be seen to reside in the pore spaces between the larger diamond crystals (Fig. 2). Several scientists (Zhutong et al. 1983; Hong et al. 1991; Britun et al. 1992) have described similar accumulations of fine-grained particles within coarse-grained joints in sintered diamond samples. The starting diamond grains are fractured when subjected to high pressure, and the resulting fragments fill in openings between the grains.

The diamond grain boundaries in the sintered compact at 1200 °C (Fig. 1a) and at 1600 °C (Fig. 1b) were tightly joined. However, even the compact sintered at 1600 °C revealed pore spaces containing diamond crystallites on the order of 0.1-0.3 μm in size. Electron diffraction of neighboring grains suggested that relative particle orientation was random. The diamond grains

Table 1. Conditions for sintering experiments

P (GPa)	*T* (°C)	Time (h)	Grain size (μm)
6	1200	6	5–7
6	1200	Blow-out*	4–8
6	1600	0.2	5–7
6	1600	0.5	5–7
6	1600	1.3	4–8
6	1600	2	5–7
6	1600	2	4–8
6	1600	3	5–7
6	1600	6	5–7
6	1800	Blow-out*	5–7
8	1200	2	5–7
8	1600	6	5–7
8	1800	6	4–8

* Blow outs are experiments in which the pressure in the system dropped below a predetermined limit in the program used in the operation of the multi-anvil press because of a defect in the internal sample assembly system.

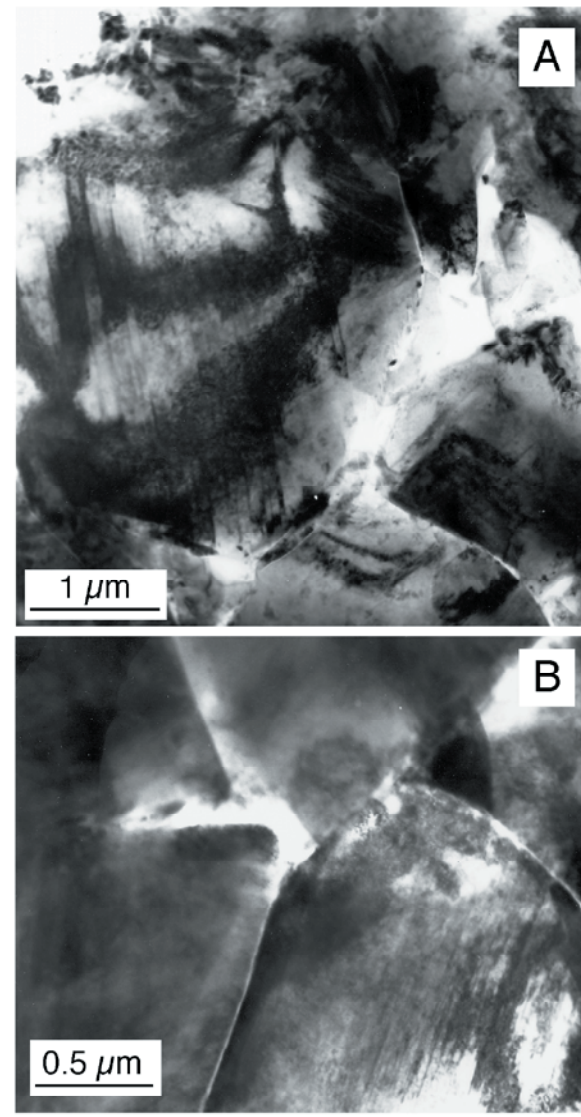

Figure 1. Bright field images of diamond grains in the compacts after sintering at (**a**) 1200 °C and 6 GPa and (**b**) 1600 °C and 6 GPa.

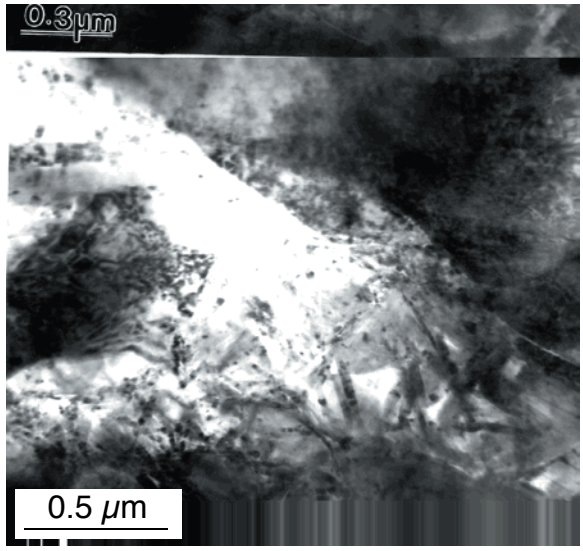

FIGURE 2. Acicular diamond crystals filling spaces between larger diamond grains.

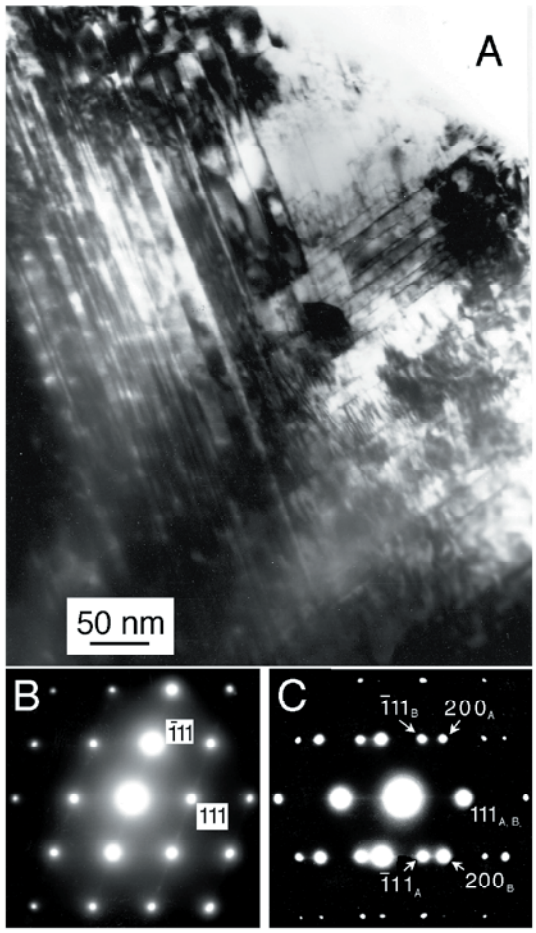

FIGURE 3. (**a**) Intersecting sets of planar defects in a diamond grain from a compact sintered at 1200 °C and 6 GPa; (**b**) SAED patterns of certain areas reveal faint streaking parallel to <111>*; (**c**) composite SAED pattern indicates spinel twinning.

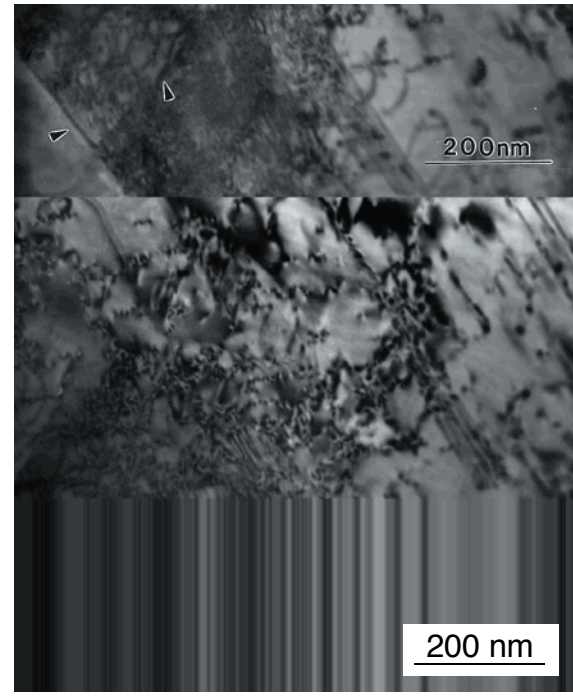

FIGURE 4. Braided dislocations in diamond grains sintered at 1200 °C and 6 GPa.

annealed at 1200 °C showed two sets of planar defect lamellae intersecting at an angle of 71° (Fig. 3a). The periodicity of the planar defects varied from 3 to 30 nm. In some instances, one set of planar defects enclosed a second set of the other orientation. This second set usually was not as clearly defined. Diffraction patterns of regions with two sets of planar defects showed faint streaking along the <111>* directions (Fig. 3b), as is consistent with the angle between the traces of the planar defects observed in the bright field images.

Selected area electron diffraction (SAED) of some grains produced composite patterns (Fig. 3c), which we attribute to spinel-type twins. Twins that obey the spinel law are related by a twofold rotation about <111> with {111} serving as the composition plane, and they are the most common twin type observed in diamond (Harlow 1998). High-density tangles of line defects accompany the planar defects in some grains (Fig. 4). In the diamond grains annealed at 1600 °C, the periodicity of the planar defects ranged from 2.5 to 35 nm. Again, bright-field images revealed two sets of planar defect lamellae at 71° to each other, and diffraction patterns showed streaking along the <111>* directions. High resolution TEM images along [0$\bar{1}$1] (Fig. 5) clearly show that the (111) lattice fringes kink substantially as they intersect the planar defects.

In some regions, the lattice fringes adopt a "herring-bone"-like texture (arrowed in Fig. 5a), which we interpret as localized mechanical twinning according to the spinel law. This conclusion is consistent with diffraction patterns from these regions that contain a second set of diffractions related to the primary set by a twofold rotation about [111]. In addition, irregular superstructures in deformed slip zones between low-defect blocks are also

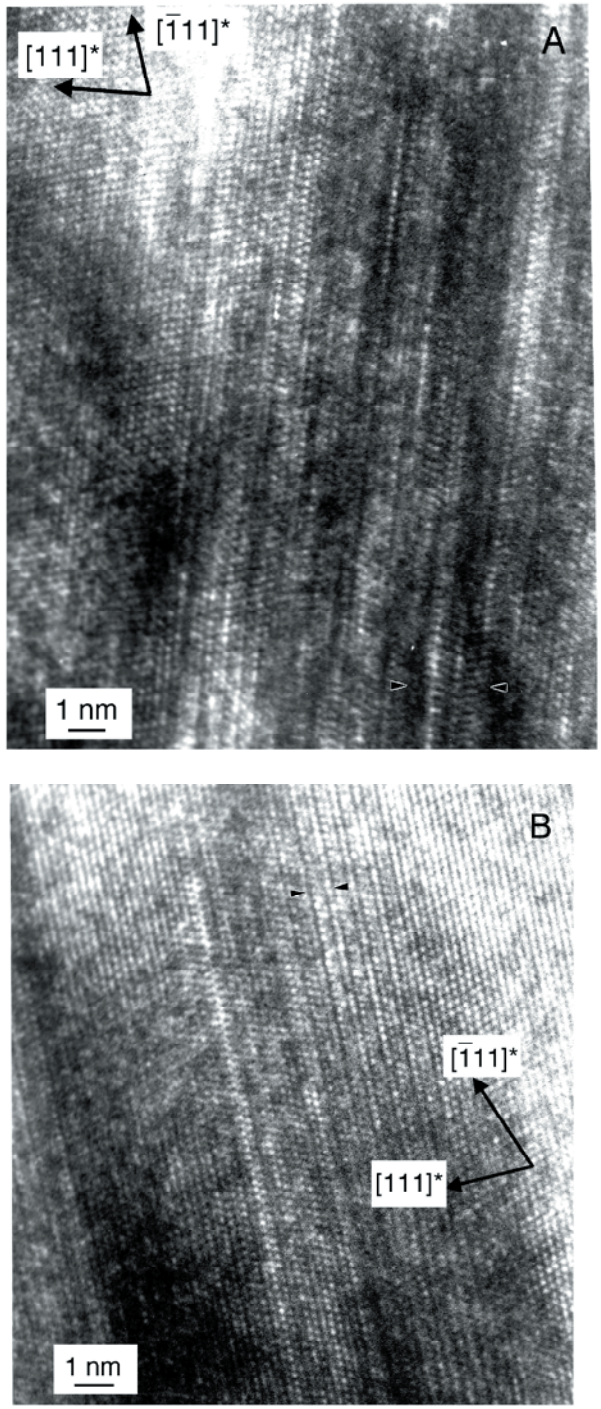

FIGURE 5. HRTEM images along [0$\bar{1}$1] exhibit "herring-bone" lattice fringe textures (between arrows) that correspond to spinel microtwins (**a**) and doubled lattice fringes indicative of localized superstructures (**b**).

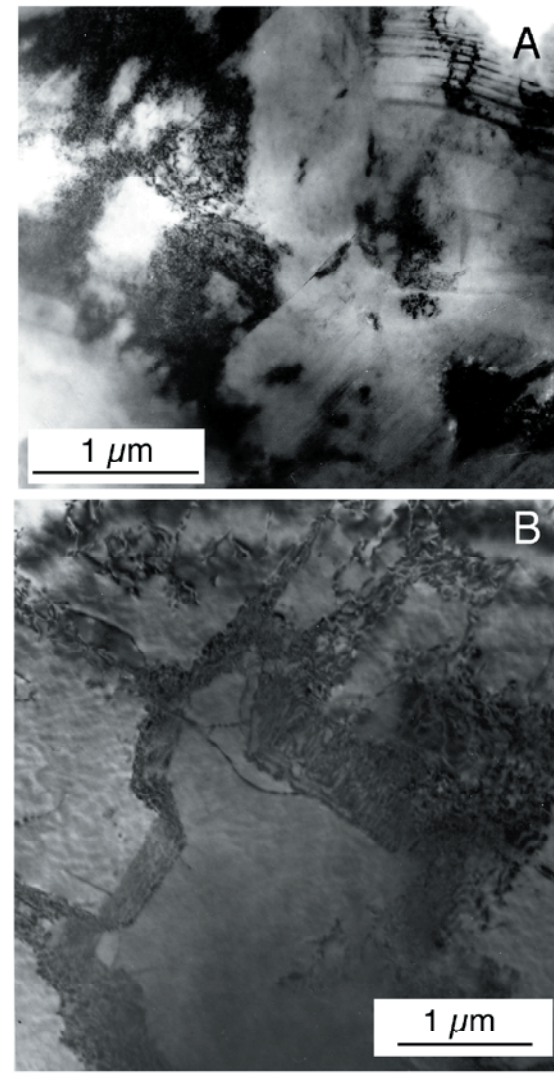

FIGURE 6. A comparison of polygonalized grain boundaries in diamond grains sintered at 8 GPa and 1200 °C (**a**) and in a natural Brazilian carbonado (**b**).

apparent in high-resolution images (Fig. 5b). As with the samples sintered at 1200 °C, bright-field TEM images revealed that one set of defect planes often enclosed a second set at 71° to the lamellar boundary of the first set. However, in the samples sintered at 1600 °C, the secondary lamellae were better developed and more conspicuous than the analogous lamellae observed in samples sintered at 1200 °C. These secondary defect lamellae were equidistant at ~28 nm, and the lamellar boundaries were thinner (~7 nm thick) than those of the primary defect lamellae.

Variations in microstructures with pressure

No published studies have thoroughly explored the effects of pressure on the sintering process in diamond. We conducted two successful experiments at 1200 °C with pressures of 6 and 8 GPa. Although the sintering times were different, we can still offer some interpretations regarding the evolution of microstructures in these diamond samples.

The starting diamond powders had grain sizes of 5 to 7 μm, and the final grain sizes of the sintered diamonds in both experiments ranged from 0.5 to 2.5 μm. Unlike diamonds sintered at 6 GPa, the compacts compressed at 8 GPa exhibited euhedral

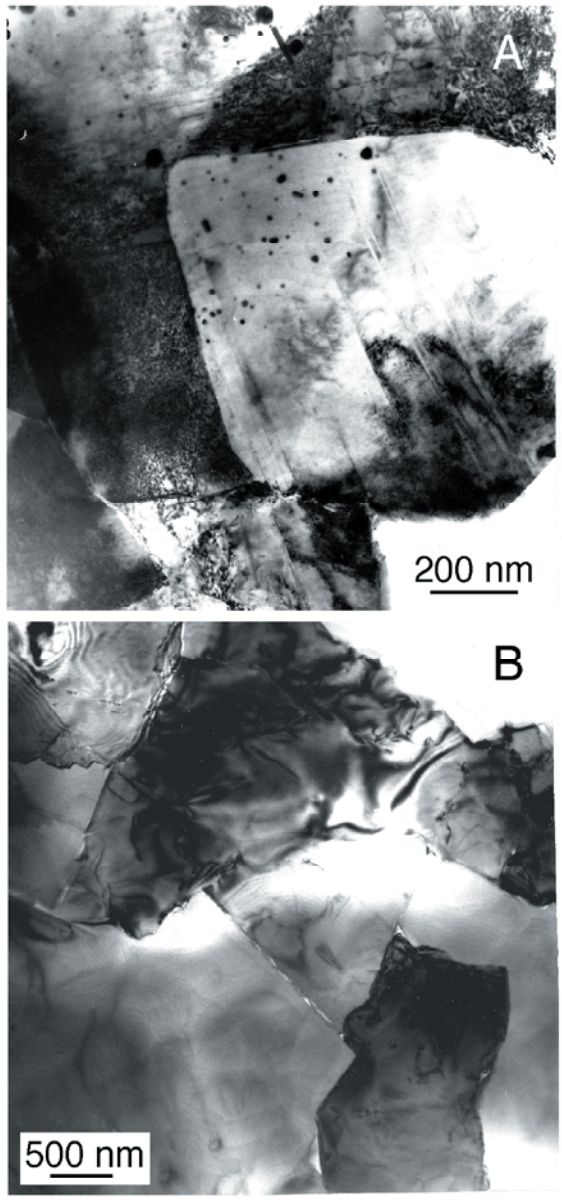

FIGURE 7. (**a**) Bright-field TEM images of a euhedral diamond with comparatively low dislocation densities in a compact sintered at 8 GPa and 1200 °C for 2 h. (**b**) Bright-field TEM images of subhedral diamonds within the fine-grained matrix of a natural Central African carbonado.

crystals with very low dislocation densities surrounded by grains in which dislocation densities were quite high (Fig. 6a). This observation implies that these higher pressure conditions allowed diamond to anneal. The resulting textures were somewhat reminiscent of the polygonalized networks observed in natural carbonado specimens (Fig. 6b). The grain boundaries of the euhedral crystals in the sintered compact (Fig. 7a) are extensively flat planar, and in this regard, they also are similar to those observed in the low-defect subhedral diamond grains of carbonado (Fig. 7b).

As with the diamonds sintered over a range of temperatures, the diamonds sintered in this set of experiments exhibited two

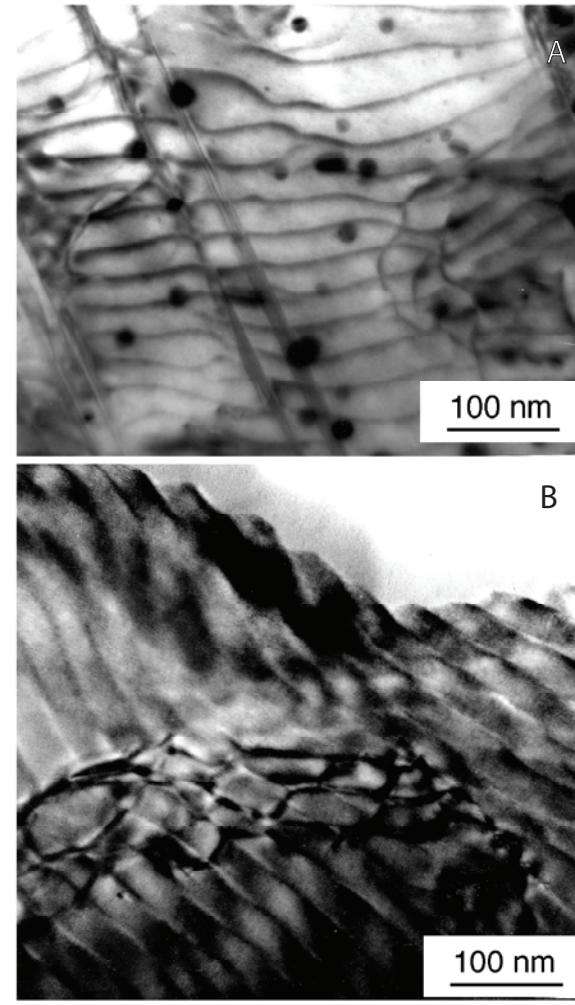

FIGURE 8. Curviplanar defect lamellae in diamond grains sintered at 8 GPa and 1200 °C (**a**) are reminiscent of defects pervasive in natural Central African carbonado (**b**).

groups of planar defects intersecting at 71°. The distance between the defect planes ranged from 7 to 40 nm. Diffraction patterns of areas containing both sets of planar defects show very faint streaking along two <111>* directions.

Additionally, the sintered diamond compact at the higher pressure of 8 GPa displayed a style of defect lamellae that was distinct from the defects oriented strictly parallel to {111}. As seen in Figure 8a, these planar defects exhibit slightly curvaceous boundaries and are highly periodic, with wavelengths of ~30 nm. The distance between defect boundaries was also greater than that observed for the flat planar defects. However, diffraction patterns across these defects did not show any streaking, and overall these microstructures strongly resembled the defect lamellae that we have observed in carbonado (Fig. 8b) (De et al. 1998). It is difficult to determine whether the flat planar defects formed before the curvaceous defect lamellae or vice-versa, though the curvaceous defect lamellae do alter their orientations slightly at the boundaries of planar defects, suggesting that the latter nucleated after the curvaceous boundaries.

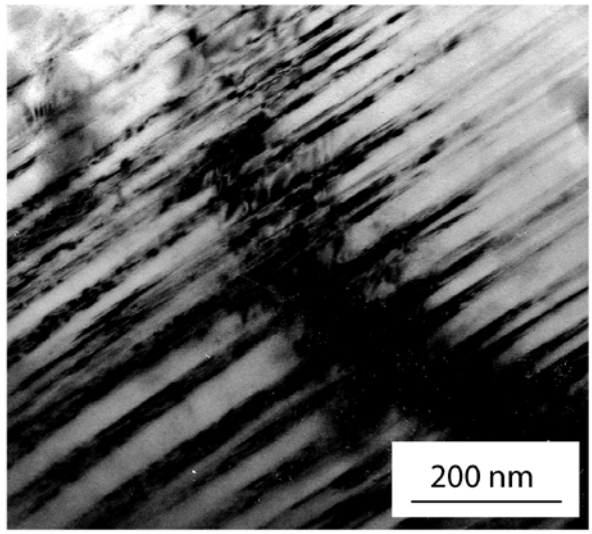

FIGURE 9. Planar defects in diamond grains sintered at 6 GPa, 1600 °C, and 3 h.

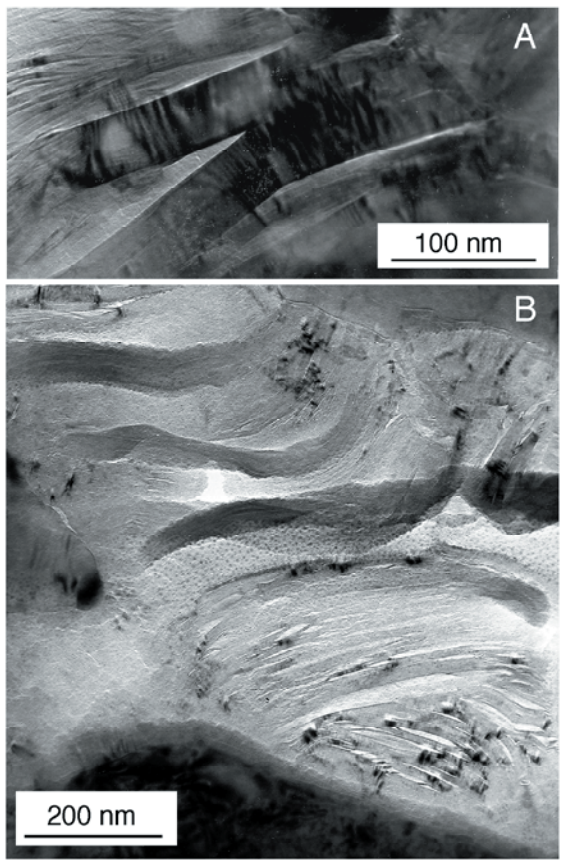

FIGURE 10. Rapid depressurization during "blow-out" episodes produced diamonds with anastomosing graphite cleavage fabrics (**a**) as fracture fills (**b**).

The sintered diamond compact annealed at 1200 °C and 8 GPa also revealed twin textures as was confirmed with SAED across the twin boundaries. Bright field images of the twins appeared very similar to images of regions separated by the flat planar defects, except that the width of the twin lamellae ranged from 200 to 800 nm, whereas the planar defects were separated by less than 100 nm

Variation in microstructures as a function of sintering times

We examined sintered diamond products from three experiments conducted at 1600 °C, 6 GPa, and times of 2, 3, and 6 h. The initial grain size for all of these experiments was 5 to 7 μm. The grain sizes of the sintered compact after 2, 3, and 6 h were 0.4 to 2 μm, 1 to 5 μm, and 0.2 to 4 μm, respectively. Thus, the grain sizes of the resultant sintered compacts showed little variation. The concentrations of randomly oriented dislocations decreased as the sintering time increased. However, the changes in the density and characteristics of planar defects with changes in time are more difficult to distinguish.

Britun et al. (1992) sintered diamond powders of two grain sizes, 5 to 7 μm and 28 to 40 μm, at a pressure of 7.7 GPa in the temperature range of 700 to 2500 °C for times of 30 and 60 s. The authors observed scattered dislocations as well as single twins only in the experimental products with initial grain sizes of 28 to 40 μm, not in the compacts produced from the smaller diamond grains. However, our experiments generated planar defects and random dislocations in samples with initial grain sizes of 4 to 8 μm and 5 to 7 μm annealed at 1200 °C and 1600 °C. We believe that the generation of defects in smaller grains might be the result of the longer times involved in our experiments.

After annealing at 2 h, diamond grains developed somewhat periodic planar defects separated by 15 to 300 nm, and weak streaking was observed in diffraction patterns along <111>*. Selected area electron diffraction of regions measuring 10 μm in diameter revealed that these planar defects were predominantly spinel-type twin boundaries. The nearly equal intensities of the two diffraction sets suggest similar abundances of the two twin components.

By contrast, diamond grains annealed for longer times of 3 and 6 h did not reveal any diffraction evidence for twins, but the diffraction patterns did exhibit strong streaking along <111>* due to planar defects separated by 10 to 50 nm (Fig. 9). These results suggest that twins anneal more readily than stacking faults, though additional experiments are needed to confirm this interpretation.

Interestingly, two of our experiments resulted in "blow-outs" in which the system pressure dropped below a predetermined limit in the program used in the operation of the multi-anvil press because of a defect in the internal sample assembly system. One of the samples produced by this extremely rapid depressurization was studied by TEM (Fig. 10). Bright-field images of layered packets measuring ~50 μm in thickness suggested that the precursor diamond had transformed to graphite, as was confirmed by measurements of faint but distinct rings in SAED patterns of the samples.

DISCUSSION

Did our sintering experiments successfully replicate carbonado? Some of the microstructures of the sintered compact produced at 8 GPa, 1200 °C, and 2 h were very similar to those observed in carbonado. For example, the curviplanar defects

characteristic of carbonado were replicated only in this experiment (Fig. 8). These curviplanar defect lamellae appear to differ from the flat-planar defects observed in other natural polycrystalline diamond varieties such as framesite (DeVries 1973) and in previously published descriptions of artificial polycrystalline compacts (Walmsley and Lang 1983, 1988; Britun et al. 1992), including those seen in low *P-T* compacts in our own work (Fig. 3a). They are smaller in scale, more rigorously periodic, and less strongly constrained to the {111} orientation (De et al. 1998). In addition, the HRTEM images, SAED patterns, and extensive dark field analyses of the lamellar boundaries in carbonado did not reveal systematic changes in phase contrast. All of these electron microscopic observations led De et al. (1998) to conclude that these curviplanar defect lamellae in carbonado were not twins, but rather slip planes.

We infer that the microtwins and planar defects displayed by our sintered diamond compacts were produced by the mechanism outlined in Britun et al. (1992). These authors propose that local plastic deformation in regions of particle contact give rise to very high dislocation densities in the grain contact zone. The sliding of perfect dislocations and Shockley partial dislocations (SPDs) give rise to defects in the sintered diamond grains. SPD generation is usually an ordered deformation and results in microtwinning. Basal sliding with SPD participation in only one system of parallel planes (for example, {111}) results in microlamellar structure formation. Although spinel twins and flat-planar defects are extremely common in synthetically sintered diamond compacts, they are much rarer in natural carbonado.

We also noted that the diamond grains exposed to our highest pressure synthesis conditions (8 GPa, 1200 °C, and 2 h) exhibited polygonalization networks similar to those seen in carbonado. Polygonalization in the sintered compact outlines subgrains of various sizes with the largest being about 1.0 μm in diameter (Fig. 6b). In carbonado, polygonalization networks that outline subgrains within the diamond matrix range from 1.0 to 10.0 μm in diameter (Fig. 7a). The diamond grains in both carbonado and the sintered compact are randomly oriented, at least on the local scale observable by the TEM, as revealed by diffraction patterns across the subgrain boundaries.

The high-pressure sintered compacts also display something approximating the microporphyritic texture seen in carbonado. This bimodal grain size in carbonado has been confirmed for many, though not all, carbonado specimens by a host of techniques, including light optical and electron microscopy and cathodoluminescence imaging (Trueb and de Wys 1971; Shelkov et al. 1995, 1997; De et al. 1998; Magee and Taylor 1998). When microporphyritic textures are present, the larger euhedral diamond crystals exhibit low dislocation densities, whereas the dislocation density in the matrix is greater than 10^{12} cm^{-2} (De et al. 1998). In the sintered compact, we observed similar euhedral crystals with very low dislocation densities (Fig. 7a) enveloped within a fine-grained diamond matrix having a very high dislocation density.

Even though the grains in both carbonado and the sintered diamond compacts (at 1600 °C and different pressures) were randomly oriented, the presence of gaps and small crystals between larger diamond grains in the sintered diamond suggests that our synthetic compacts did not reproduce the toughness of carbonado. Although carbonado exhibits porosity at the macroscopic scale (with vugs measuring hundreds of micrometers to several millimeters in diameter), individual grains are so tightly bonded that finer scale porosity between crystals is not apparent.

Based on the absence of microstructures characteristic of carbonado (such as defect lamellae, polygonalization networks, and porphyritic textures) in sintered diamond compacts at 6 GPa (at different temperatures), one might argue that their production at 8 GPa places a constraint on the pressure that carbonado experienced during its genesis. However, even at the higher pressure of 8 GPa, we observed other defects in the sintered diamond (parallel slip planes, spinel type twins, nested planar defects) that we have not observed in carbonado. Our results lead us to believe that under our experimental conditions we were not successful in replicating natural carbonado.

Nevertheless, the production of the curviplanar defects and the polygonalization textures strongly suggest that these kinds of experiments may yet succeed in generating a synthetic analog of carbonado. The fact that these textures *can* form in quasi-hydrostatic high-pressure experiments (and that very different microstructures are produced during the rapid depressurization attending blow-outs) suggests that these microstructures do not require an impact scenario for their generation, as we suggested previously (De et al. 1998). In turn, this inference may lend weight to models for carbonado genesis that invoke an origin in the mantle. Still, we remain puzzled by the absence of mantle phase inclusions in carbonado (Trueb and de Wys 1971; De et al. 1998) and by the many suggestions that carbonado diamond formed from organic carbon; this evidence would include the narrow $\delta^{13}C$ distributions near –26‰ for Brazilian and CAR carbonado specimens (Shelkov et al. 1997; De et al. 2001) and a recent analysis of N-V defect centers (Nadolinny et al. 2003). Knowing whether carbonado-like defect assemblages can also be generated during an impact event awaits a TEM examination of diamond compacts produced by well-constrained shock-metamorphism experiments.

Acknowledgments

We thank J. Konzett, W. Minarik, and J. Li for their help with the diamond synthesis experiments. We are grateful to Y. Kagi and T. Daulton for their detailed reviews of this paper. S. De also thanks the Carnegie Institution and the Geophysical Laboratory for the pre-doctoral fellowship that supported this study. We also thank T. Rusnack for TEM assistance. This work was supported by NSF grants EAR97-06143 and EAR00-73862.

References cited

Angus, J.C. and Hayman, C.C. (1988) Low-pressure metastable growth of diamond and "diamondlike" phases. Science, 241, 913–921.

Bertka, C.M. and Fei, Y. (1996) Constraints on the mineralogy of an iron-rich Martian mantle from high pressure experiments. Planetary and Space Science, 44, 1269–1276.

——— (1997) Mineralogy of the Martian interior up to core-mantle boundary pressures. Journal of Geophysical Research, 102, 5251–5264.

Britun, V.F., Oleynik, G.S., and Semenenko, N.P. (1992) Deformation processes during high-pressure sintering of the diamond powders produced by catalytic synthesis. Journal of Materials Science, 27, 4472–4476.

Bundy, F.P. (1962) Direct conversion of graphite to diamond in static pressure apparatus. Science, 137, 1057–1058.

——— (1974) Superhard Materials. Scientific American, 231, 62–70.

Bundy, F.P., Hall, H.T., Strong, H.M., and Wentorf, R.H. (1955) Man-made diamonds. Nature, 176, 51–55.

De, S., Heaney, P.J., Hargraves, R.B., Vicenzi, E.P., and Taylor, P.T. (1998) Microstructural observations of polycrystalline diamond: a contribution to the carbonado conundrum. Earth and Planetary Science Letters, 164, 421–433.

De, S., Heaney, P.J., Vicenzi, E.P., and Wang, J. (2001) Chemical heterogeneity in

carbonado, an enigmatic polycrystalline diamond. Earth and Planetary Science Letters, 185, 315–330.
DeCarli, P.S. (1995) Shock wave synthesis of diamond and other phases. Material Research Society Symposium Proceedings, 383, 21–31.
——— (1998) Direct synthesis of diamond in the laboratory and in impact structures. Meteoritics and Planetary Science, 33, A39 (Supplement).
DeVries, R.C. (1973) Evidence for plastic deformation in the natural polycrystalline diamond, framesite. Material Research Bulletin, 8, 733–742.
DeVries, R.C., Badzian, A., and Roy, R. (1996) Diamond synthesis: The Russian connection. Materials Research Society Bulletin, 21, 65–75.
Dismukes, J.P., Gaines, P.R., Witzke, H., Leta, D.P., Kear, B.H., and Behal, S.K. (1988) Demineralization and microstructure of carbonado. Material Science and Engineering, A(105/106), 555–563.
Frantesson, Y.V. and Kaminsky, F.V. (1974) Carbonado, a diamond variety of nonkimberlitic origin. Transactions (Doklady) of the U.S.S.R. Academy of Sciences: Earth Science Sections, 219, 117–119.
Giardini, A.A. and Tydings, J.E. (1962) Diamond synthesis: Observations on the mechanism of formation. American Mineralogist, 47, 1393–1421.
Haggerty, S.E. (1996) Diamond-carbonado: models for a new meteorite class of circumstellar or solar system origin. EOS, 77, S143.
Hall, T.H. (1970) Sintered diamond: A synthetic carbonado. Science, 169, 868–869.
Harlow, G.E., Ed. (1998) The Nature of Diamonds. Cambridge University Press: Cambridge.
Hong, S., Akaishi, M., Kanda, H., Osawa, T., and Yamaoka, S. (1991) Dissolution behavior of fine particles of diamond under high pressure sintering conditions. Journal of Materials Science Letters, 10, 164–166.
Hornstra, J. (1957) Dislocations in diamond lattice. Journal of the Physics and Chemistry of Solids, 5, 129–141.
Irifune, T., Kurio, A., Sakamoto, S., Inoue T., Sumiya, H. (2003) Ultrahard polycrystalline diamond from graphite. Nature, 421, 599–600.
Jeynes, C. (1978) Natural polycrystalline diamond. Industrial Diamond Review, January, 15–28.
Kagi, H., Takahashi, K., Hidaka, H., and Masuda, A. (1994) Chemical properties of Central African carbonado and its genetic implication. Geochimica et Cosmochimica Acta, 58, 2629–2638.
Klages, C.P. (1995) Metastable diamond synthesis-principles and applications. European Journal of Mineralogy, 7, 767–774.
Lammer, A. (1988) Mechanical Properties of polycrystalline diamond. Materials Science and Technology, 4, 949–955.
Liander, H. and Lundblad, E. (1960) Some observations on the synthesis of diamonds. Arkiv foer Kemi, 16, 139–149.
Magee, C.W. and Taylor, W.R. (1998) Constraints on the history and origin of carbonado from luminescence studies. Seventh International Kimberlite Conference, Extended Abstracts, 527–528, Cape Town, South Africa.
Nadolinny, V.A., Shatsky, V.S., Sobolev, N.V., Twitchen, D.J., Yuryeva, O.P., Vasilevsky, L.A., and Lebedev, V.N. (2003) Observation and interpretation of paramagnetic defects in Brazilian and Central African carboandos. American Mineralogist, 88, 11–17.
Naka, S., Horii, K., Takeda, Y., and Fanawa, T. (1976) Direct conversion of graphite to diamond under static pressure. Nature, 259, 38–39.
Ozima, M. and Tatsumoto, M. (1997) Radiation-induced diamond crystallization: Origin of carbonados and its implications on meteorite nanodiamonds. Geochimica Cosmochimica Acta, 61, 369–376.
Ozima, M., Zashu, S., Tomura, K., and Matsuhisa, Y. (1991) Constraints from noble-gas contents on the origin of carbonado diamonds. Nature, 351, 472–474.
Shelkov, D., Verchovsky, A.B., Pillinger, C.T., Hutchison, R., and Milledge, H.J. (1995) Carbonado: More clues to a common impact origin for samples from Brazil and the Central African Republic. Lunar and Planetary Science Abstracts, 26, 1281–1282.
Shelkov, D., Verkhovsky, A.B., Milledge, H.J., and Pillinger, C.T. (1997) Carbonado: A comparison between Brazilian and Ubangui sources with other forms of microcrystalline diamond based on carbon and nitrogen isotopes. Russian Geology and Geophysics, 38, 332–340.
Shelkov, D.A., Verchovsky, A.B., Milledge, H.J., Kaminsky, F.V., and Pillinger, C.T. (1998) Carbon, nitrogen, argon and helium study of impact diamonds from Ebeliakh alluvial deposits and Popigai crater. Meterotics and Planetary Science, 33, 985–992.
Slobodskoi, V.Y., Sobolev, V.V., and Baranov, P.N. (1990) Diamond crystallization mechanisms. Fizika Goreniya i Vzryva, 26, 119–122.
Smith, J.V. and Dawson, J.B. (1985) Carbonado: Diamond aggregates from early impacts of crustal rocks? Geology, 13, 342–343.
Trueb, L.F. and de Wys, E.C. (1971) Carbon from Ubangi—Microstructural study. American Mineralogist, 56, 1252–1268.
Walmsley, J.C. and Lang, A.R. (1983) Transmission electron microscopic observations of deformation and microtwinning in a synthetic diamond compact. Journal of Materials Science Letters, 2, 785–788.
——— (1988) Characteristics of diamond regrowth in a synthetic diamond compact. Journal of Materials Science, 23, 1829–1834.
Wentorf, R.H., Devries, R.C., and Bundy, F.P. (1980) Sintered superhard materials. Science, 208, 873–880.
Williams, B.E., and Glass, J.T. (1989) Characterization of diamond thin films: Diamond phase identification, surface morphology, and defect structures. Journal of Materials Research, 4, 373–384.
Yazu, S., Nishikawa, T., Nakai, T., and Doi, Y. (1983) TEM observation of microstructures of sintered diamond compacts. In N.R. Comins, Ed., Proceedings of the International Conference on Recent Developments in Specialty Steels and Hard Materials, p. 449. Pergamon Press, Oxford.
Yu, H. and Li, S. (1994) Sintering of ultrafine diamond particles under high temperature and high pressure. Diamond and Related Materials, 3, 222–226.
Zhang, Y., Zhang, F., and Chen, G. (1994) A study of the pressure-temperature conditions for diamond growth. Journal of Materials Research, 9, 2845.
Zhutong, S., Dayu, Y., and Guoxiang, S. (1983) The microstructures of synthetic diamonds. Kexue Tongbao, 28, 24–29.

MANUSCRIPT RECEIVED FEBRUARY 3, 2003
MANUSCRIPT ACCEPTED AUGUST 19, 2003
MANUSCRIPT HANDLED BY ALISON PAWLEY